



Technical Report

The rapid $A-C_i$ response: photosynthesis in the phenomic eraJoseph R. Stinziano^{1,2} , Patrick B. Morgan^{3,4}, Douglas J. Lynch³, Aaron J. Saathoff^{3,4}, Dayle K. McDermitt³ & David T. Hanson¹ ¹Department of Biology, The University of New Mexico, Albuquerque, NM 87104, USA, ²Department of Biology, The University of Western Ontario, London, Ontario, N6A 5B7, Canada, ³LI-COR Inc., Lincoln, NE 68504, USA and ⁴School of Natural Resources, University of Nebraska–Lincoln, Lincoln, NE 68583, USA

ABSTRACT

Phenotyping for photosynthetic gas exchange parameters is limiting our ability to select plants for enhanced photosynthetic carbon gain and to assess plant function in current and future natural environments. This is due, in part, to the time required to generate estimates of the maximum rate of ribulose-1,5-bisphosphate carboxylase oxygenase (Rubisco) carboxylation ($V_{c,max}$) and the maximal rate of electron transport (J_{max}) from the response of photosynthesis (A) to the CO_2 concentration inside leaf air spaces (C_i). To relieve this bottleneck, we developed a method for rapid photosynthetic carbon assimilation CO_2 responses [rapid $A-C_i$ response (RACiR)] utilizing non-steady-state measurements of gas exchange. Using high temporal resolution measurements under rapidly changing CO_2 concentrations, we show that RACiR techniques can obtain measures of $V_{c,max}$ and J_{max} in ~5 min, and possibly even faster. This is a small fraction of the time required for even the most advanced gas exchange instrumentation. The RACiR technique, owing to its increased throughput, will allow for more rapid screening of crops, mutants and populations of plants in natural environments, bringing gas exchange into the phenomic era.

Key-words: $A-C_i$; C_3 ; carboxylation; CO_2 ; gas exchange; phenotyping; photosynthesis.

INTRODUCTION

We are in an era where our ability to assess physiological function is limiting throughput in screening for desired traits in plants (Furbank & Tester 2011; Araus *et al.* 2014). This has implications for food security and biofuel production, such as the development of crops with improved photosynthetic performance or water use efficiency to boost yields for adequate food production by 2050 (Ray *et al.* 2013). The need to overcome this limitation has spawned phenomics – large-scale screening of plant phenotypes (e.g. Lobos *et al.* 2014). Most phenomic platforms rely on imaging (Furbank & Tester 2011), which can be powerful but are challenging to operate in the field. Furthermore, it is critical that they generate new fundamental data describing useful parameters of photosynthetic function, such as $V_{c,max}$ [the maximum rate of ribulose-1,5-bisphosphate carboxylase oxygenase (Rubisco)

carboxylation] and J_{max} (the maximal rate of electron transport). These two parameters are essential for the foundational Farquhar *et al.* (1980) model (FvCB) that relates photosynthetic biochemistry to prevailing environmental conditions (von Caemmerer 2013). This model has also been embedded into earth system models, and uncertainty in $V_{c,max}$ has been identified as a major source of error (Rogers 2014). Accelerating our ability to screen for photosynthetic gas exchange traits such as $V_{c,max}$ will help to achieve improvements in crop yields and in modelling climate change. Recent advances in hyperspectral reflectance are generating high-throughput parameters that correlate fairly well with $V_{c,max}$ (Serbin *et al.* 2015; Yendrek *et al.* 2016), but their mechanistic foundation and assumptions differ greatly from the ‘gold standard’ gas exchange approach.

Photosynthetic traits are screened several ways, including point measurements of net CO_2 assimilation rates (A , ~1 to 5 min per measurement, depending on the system), photosynthetic light response curves (~10 to 30 min, depending on the system and number of irradiances) and photosynthetic CO_2 response curves (~30 to 60 min, depending on system and number of concentrations). Point measurements yield the least information, as rates of photosynthesis cannot be disentangled from daytime respiratory rates, but they can be used to screen ~100 plants per day per machine to obtain information on water use efficiency, stomatal conductance and the balance between photosynthesis and night-time respiration (e.g. Limousin *et al.* 2013; Bishop *et al.* 2015). Light response curves provide more mechanistic information such as the quantum yield (Long & Hällgren 1993) and light saturation of photosynthesis, which can be used in scaling photosynthetic rates through a canopy (Kull & Kruijt 1998; Duursma & Medlyn 2012); however, the number of plants that can be screened drops to a few tens of individuals per day. Photosynthetic carbon assimilation CO_2 response ($A-C_i$) curves can provide mechanistic information about the underlying biochemical limitations of carbon assimilation that can vary by genotype. This information can be easily assimilated into models of both plant growth and global vegetation (Farquhar *et al.* 1980; Duursma & Medlyn 2012; Oleson *et al.* 2013), but data collection is limited to a few plants per day. While $A-C_i$ curves can provide estimates of $V_{c,max}$ and J_{max} , along with other valuable information on carbon fluxes in the plant (Sharkey *et al.* 2007), the time required to execute this technique has limited utility in the context of large-scale screens. The power and utility of the $A-C_i$ curve would greatly increase if it could be carried out on a faster timescale.

Correspondence: D. T. Hanson. e-mail: dthanson@unm.edu

The FvCB model is a steady-state model used to interpret A–C_i responses (Farquhar *et al.* 1980). As generally practised, A–C_i response curves are constructed by allowing a few minutes for a leaf and gas exchange system to reach a steady state at each new [CO₂] (e.g. Long & Bernacchi 2003), but not only is this approach slow, it also allows time for complications to arise from biological responses, such as changes in enzyme activation state, chloroplast movement or stomatal aperture. Efforts in the last 10 years have focused almost entirely on optimizing fits for steady-state data collected on the minutes timescale per [CO₂] (Ethier & Livingston 2004; Sharkey *et al.* 2007; Gu *et al.* 2010; Duursma 2015; Bellasio *et al.* 2016a, 2016b), not on developing new gas exchange methods to increase throughput. An early alternative approach to performing A–C_i curves was proposed by Davis *et al.* (1987) who showed such curves could be measured with a closed, transient photosynthesis system using a continuous drawdown method in which chamber [CO₂] was continuously depleted by a leaf sample held in a closed assimilation chamber. Later, McDermitt *et al.* (1989) demonstrated that A–C_i curves measured on soybean leaves by continuous drawdown in which [CO₂] changed at rates of 0.01 to 1 $\mu\text{mol mol}^{-1} \text{s}^{-1}$ were not significantly different from those measured independently using an open, steady-state system in which soybean leaves were equilibrated for 5 min at each new [CO₂]. However, closed photosynthesis systems can introduce significant changes in temperature, pressure and water vapour if not controlled by recirculation (Long & Hällgren 1993). Furthermore, Laisk & Oja (1998) showed that CO₂ diffusion into a leaf followed by solvation and Rubisco carboxylation came into apparent steady state with large step changes in external [CO₂] in ~1 s or less, making it possible to measure Rubisco kinetic parameters *in vivo* that were in good agreement with values measured *in vitro*. These results suggest that plant leaves quickly come into at least a quasi steady state with changing [CO₂] in the air around them, suggesting it is possible to use a continuously variable approach for generating A–C_i response curves to generate parameters for use in the FvCB steady-state model.

Here we present a rapid A–C_i response (RACiR) technique that reduces the time necessary to determine an A–C_i response to ~5 min (or possibly faster), making it theoretically possible to screen hundreds of plants over several days with a single instrument. The RACiR technique takes advantage of technological advancements that allow measurement of A during dynamic changes in C_i in an open gas exchange system, and it generates the same model parameters, using the same curve fitting tools as the standard A–C_i methodology. This makes it fundamentally different from other screening approaches, for example, imaging systems, that infer gas exchange parameters from correlated measurements.

METHODS

Plant material

Poplar trees (*Populus deltoides* Barr. S7c8 East Texas day neutral clone) were grown from cuttings in a greenhouse at the University of New Mexico [35.0843°N, 106.6198°W,

1587 m above sea level (a.s.l.)] at 18.3 to 21.1/15.6 to 21.1 °C day/night temperature during the month of September.

Gas exchange

Using the LI-6800 Portable Photosynthesis System equipped with the Multiphase Flash Fluorometer and Chamber (LI-COR Inc., Lincoln, NE, USA), we assessed the CO₂ response of A using two different methods: (1) traditional, steady-state A–C_i responses involving discrete, step (i.e. minutes between) changes in [CO₂] and (2) RACiRs during a CO₂ ramp (i.e. a linear change in [CO₂] at defined rates; Fig. 1 and further discussions). Chamber conditions for both methods were as follows (unless otherwise noted): fan speed of 10 000 rpm, flow rate of 600 $\mu\text{mol mol}^{-1}$, overpressure of 0.2 kPa, vapour pressure deficit (VPD) at leaf (VPD_{leaf}) of 1.2 kPa (controlled by the LI-6800), leaf temperature of 25 °C and saturating irradiance of 1000 $\mu\text{mol m}^{-2} \text{s}^{-1}$.

Traditional A–C_i response

The LI-6800 provides rapid control and measurement of stepwise changes in reference [CO₂] ([CO₂]_{ref}) and sample [CO₂] ([CO₂]_{sample}), increasing the speed at which measurements of A_{leaf} can be made. Therefore, we set the CO₂ response curve autoprogram with minimum and maximum wait times of 60 and 180 s, respectively, and matched the infrared gas analysers (IRGAs) at every CO₂ concentration. Incoming leaf chamber flow rate was set to 600 $\mu\text{mol air s}^{-1}$ and the following values of [CO₂]_{ref} were used: 400, 350, 300, 250, 200, 150, 100, 50, 400, 500, 600, 700, 800, 900, 1000, 1100, 1200, 1300, 1400, 1500, 1800 and 2000 $\mu\text{mol mol}^{-1}$. We performed these measurements on the same day and on the same leaf location as RACiR measurements and two additional times on separate days to analyse variation in estimates of V_{c,max} and J_{max} from separate curves for an individual plant. The pseudo-replicated traditional A–C_i responses were very similar across days, so we used the mean of the fits [mean V_{c,max}, J_{max} and root mean square error (RMSE)] for statistical comparisons with the RACiR method.

Rapid A–C_i response technique

An important limitation to measuring fast responses with any system is the time required to change and measure the gas concentrations in the sample and reference chambers. This is facilitated in the LI-6800 by splitting the airflow between sample and reference paths in the measurement head immediately before the flow meter, leaf chamber and IRGAs, so the times required for flows to transport chamber input and output gas concentrations to the IRGAs are very short, a few seconds. The reference and sample IRGAs report gas concentrations entering and leaving the leaf chamber with good temporal fidelity because flow-rate-dependent time delays are quite small. When incoming [CO₂] is continuously increased (or decreased), the increase (or decrease) will be measured immediately by the reference IRGA, but the sample IRGA will see a slower response because the sample chamber dilutes the

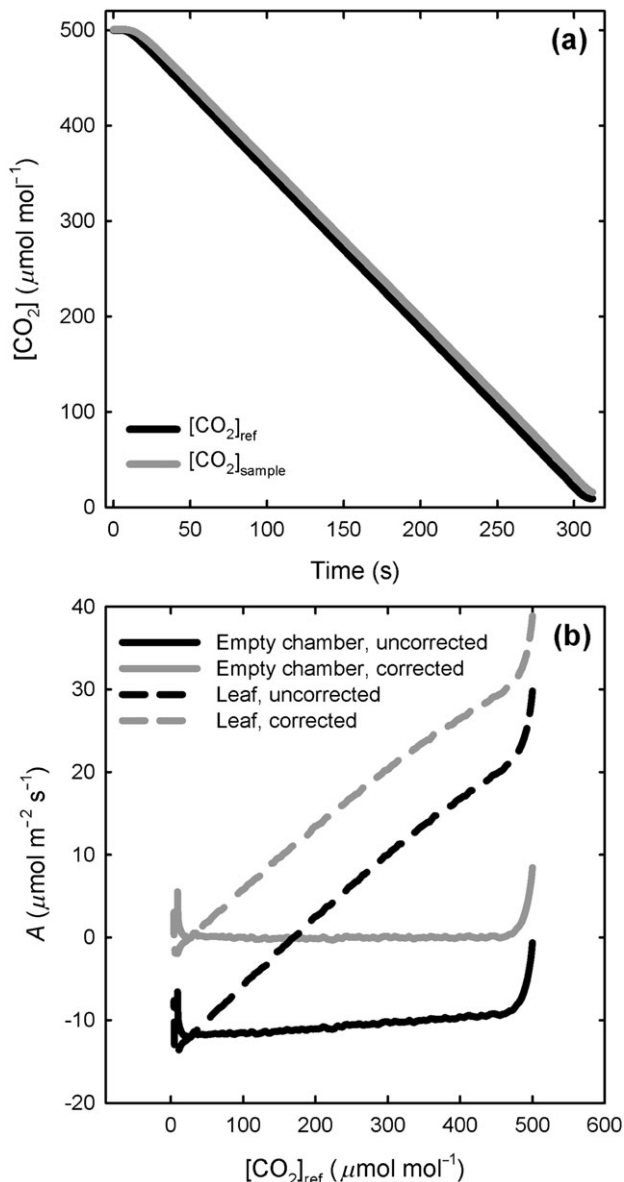


Figure 1. Rapidly changing [CO₂] causes an apparent CO₂ assimilation value that must be corrected for using an empty chamber. (a) Changes and lag between the reference ([CO₂]_{ref}) and sample ([CO₂]_{sample}) [CO₂]. (b) Example uncorrected and corrected data in a chamber with and without a leaf for *Populus deltoides*. See the supporting information for an example of how the correction was performed.

increase (or decrease) with a first-order time constant given by chamber volume divided by volumetric flow rate, which is the mean residence time in the leaf chamber. This volumetric dilution process will be complete after three to five time constants, and then, if the chamber is empty, [CO₂] in the chamber will increase (or decrease) at the same rate as the input [CO₂], although its value will be offset in time. Measured values for apparent *A* will be determined by the instantaneous [CO₂] difference measured between sample and reference IRGAs, which is due to the sum of four contributions: (1) uptake of CO₂ by a leaf, if present; (2) the amount by which the chamber

[CO₂] lags the incoming reference [CO₂] due to residence time in the chamber; (3) small IRGA match offsets that may accumulate as the reference [CO₂] increases (or decreases); and (4) any small residual errors due to flow-related time delays in transporting air to the IRGAs. The last three contributors arise from properties of the system and are similar with or without a leaf in the chamber, so they can be measured in an empty chamber test.

A correction procedure was developed to account for effects of chamber dilution, match offsets and system residual time delays. Figure 1a shows data from an experiment using an empty chamber (i.e. no leaf), during which the [CO₂]_{ref} was linearly attenuated from 500 to 0 μmol mol⁻¹ at 100 μmol mol⁻¹ min⁻¹. While changes in [CO₂]_{ref} over time were measured more or less immediately by the reference IRGA, the sample chamber acts as a mixing volume, diluting and delaying the incoming [CO₂]_{sample}. The resulting time delay is characterized by the chamber mean residence time, typically near 5 s (Fig. 1a). The result is a lag in the change in [CO₂]_{sample}, giving rise to an offset in *A* of an empty chamber (*A*_{EC}) versus [CO₂]_{ref} of around -11 μmol CO₂ m⁻² s⁻¹ (Fig. 1b, dark solid line). The linear portion of the uncorrected empty chamber data in Fig. 1b also has a slight upward slope. This is due to the accumulation of a small match offset as [CO₂]_{ref} and [CO₂]_{sample} change, and it is equivalent to about a 2 μmol CO₂ m⁻² s⁻¹ offset at its maximum extent. A third offset (not shown) resulting from residual time delays (300–600 ms at system flow rates) due to small length differences in sample and reference flow paths amounts to less than 1 μmol CO₂ m⁻² s⁻¹.

The apparent net CO₂ assimilation rate (*A*_{apparent}) is a composite of the dynamics of net assimilation by the leaf and the system kinetics and offsets just described. The system response time is determined by performing a linear regression on the response of an empty chamber to the RACiR CO₂ ramp. Data were selected only from the linear portion of the ramp after dilution transients were satisfied (Fig. 1b, dark solid line, but excluding non-linear endpoint dynamics).

$$A_{EC} = m^*[\text{CO}_2]_{\text{ref}} - b \quad (1)$$

The sign and absolute value of the slope (*m*) are a composite of the system-level characteristics just described. *A*_{leaf} was calculated using Eqn 2 by subtracting *A*_{EC} at corresponding values of [CO₂]_{ref}.

$$A_{\text{leaf}} = A_{\text{apparent}} - A_{EC} \quad (2)$$

When this procedure is applied to the empty chamber data in Fig. 1a, a relationship is obtained with mean and slope of zero (Fig. 1b, grey solid line). Equation 1 was extended to cover the entire range of *A*_{apparent}, preserving the non-linear dynamics in the result. Values of *C*_i were recalculated using *A*_{leaf}. All data outside of the range of [CO₂]_{ref} over which empty chamber results were linear were excluded from all analyses. (for example calculations, see supporting information).

When the preceding correction protocol is used, CO₂ concentrations were changed using a 100 μmol mol⁻¹ min⁻¹ linear ramp for all rapid CO₂ response curves and by controlling VPD

at 1.5 kPa, except as noted. This rate was chosen because it is an appropriate compromise between speed and data capture. The datalogging rate was 0.5 Hz. The rapid change in [CO₂] precludes matching during the leaf measurement. RACiR measurements were performed before and after (random-order) traditional measurements on the same leaves, and in the same location on each leaf.

Since the order of CO₂ concentrations affects traditional A–C_i measurements (Long & Bernacchi 2003) and because data near the inflection point of the A–C_i response have the greatest impact on curve fitting (Sharkey *et al.* 2007; Gu *et al.* 2010), the RACiR linear ramps were run for two CO₂ ranges in both increasing and decreasing directions. Each linear ramp lasted 5 min, changing [CO₂] at 100 $\mu\text{mol mol}^{-1} \text{ min}^{-1}$ starting at 500 $\mu\text{mol mol}^{-1}$ and ramping from 500 to 0 $\mu\text{mol mol}^{-1}$ (immediately followed by 0 to 500 $\mu\text{mol mol}^{-1}$ on a looped ramp) and then moving to 300 $\mu\text{mol mol}^{-1}$ and ramping from 300 to 800 $\mu\text{mol mol}^{-1}$ (immediately followed by 800 to 300 $\mu\text{mol mol}^{-1}$ on a looped ramp). Two additional subsets of the RACiR technique were tested: one set at a 200 $\mu\text{mol mol}^{-1} \text{ min}^{-1}$ linear ramp for [CO₂] from 500 to 0 $\mu\text{mol mol}^{-1}$ (2.5 min total time) and a second one from 500 to 0 $\mu\text{mol mol}^{-1}$ subset at a 100 $\mu\text{mol mol}^{-1} \text{ min}^{-1}$ linear ramp for [CO₂], but with all H₂O controls off (i.e. VPD was allowed to vary with the ambient incoming airstream).

Data analysis

All CO₂ response data were based on a sample size of six biological replicates and were fitted with the FvCB model using the plantcophys package in R graphic user interface (GUI) (Duursma 2015). Unless otherwise noted, all settings for the fitaci function were left at default settings, as these should have limited impact on the objective of this study. Statistical analyses were run using repeated-measures analyses of variance (ANOVAS) in SIGMAPLOT v.11.0 (Systat Software, Inc., San Jose, CA, USA) amongst the standard A–C_i and RACiR curves using the LI-6800 and between the 500 to 0 RACiR curves with and without VPD control, followed by Tukey's honestly significant difference (HSD). In cases where the assumptions of normality were violated, Friedman repeated-measures ANOVAS on ranks were run on the data.

RESULTS

The rapid rate of change in [CO₂] creates a difference in [CO₂] reported by the reference and sample IRGAs due to residence time and volumetric dilution in the sample chamber. Because the rate of increase in [CO₂] is kept constant, the difference between reference and sample IRGAs quickly stabilizes, typically within 20–30 s (Fig. 1a). This difference creates an apparent CO₂ assimilation value in an empty chamber (Fig. 1b) that can be corrected using a linear-regression-based approach that removes the effects of chamber residence time, IRGA match offsets and other small errors (Fig. 1b and the supporting information). Without correction for this effect, the RACiR is offset from the steady-state A–C_i response by an amount equivalent to the measured hysteresis in an empty chamber (Fig. 1b).

Once corrected, the RACiR data overlay well onto the steady-state A–C_i response (Fig. 2). We checked a few lower flow rates and found the correction still works but has a larger offset (data not shown). We did not test for a minimum flow rate.

The RACiR technique yielded data similar to the traditional A–C_i approach (Table 1). There was a significant effect of the type of rapid A–C_i curve used on RMSE of the model ($\chi^2=12.857$, d.f.=6, $P=0.045$); however, *post hoc* pairwise comparisons only yielded significant differences between the 300–800 $\mu\text{mol mol}^{-1}$ 5 min ramp and the 500–0 $\mu\text{mol mol}^{-1}$ 2.5 min ramp (Table 1). Values for the $V_{c,\text{max}}$ ($F_{6,30}=12.126$, $P<0.001$) and J_{max} ($\chi^2=20$, d.f.=6, $P=0.003$) parameters generated a few significant differences between A–C_i response types (Table 1). Post hoc pairwise comparisons indicated significant differences between the standard A–C_i curves and both the 800–300 $\mu\text{mol mol}^{-1}$ 5 min ramp and the 500–0 $\mu\text{mol mol}^{-1}$ 2.5 min ramp for J_{max} . Only the 800 to 300 $\mu\text{mol mol}^{-1}$ 5 min ramp yielded significantly lower $V_{c,\text{max}}$ estimates than the

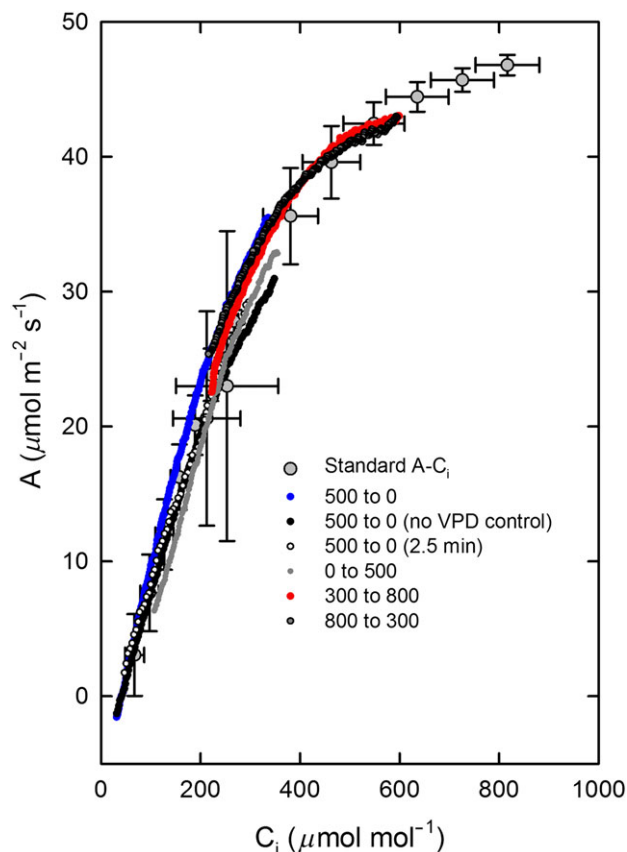


Figure 2. The rapid A–C_i response (RACiR) technique generates data that, when corrected with washout regions trimmed, overlay well onto the standard A–C_i response for *Populus deltoides*. For clarity, sample data for one individual of *P. deltoides* are shown. Data for the standard A–C_i are presented as the mean \pm standard error of the mean (s.e.m.) for three measured responses on the same leaf of a single seedling, while RACiRs were replicated once per CO₂ range per seedling on the same leaf and same location as the standard A–C_i. The best RACiRs are shown in blue (500 to 0) and red (300 to 800). See Table 1 for a statistical comparison of the RACiR and standard A–C_i response fits.

Table 1. Parameters for the $A-C_i$ responses of *Populus deltoides*

Curve type	RMSE	$V_{c,max}$ ($\mu\text{mol m}^{-2} \text{s}^{-1}$)	J_{max} ($\mu\text{mol m}^{-2} \text{s}^{-1}$)
Standard $A-C_i$ (LI-6800)	4.3 ± 0.4 a, b	119 ± 3 a, c, d, e	388 ± 42 a
500 to 0	3.1 ± 0.4 a, b	122 ± 7 a, f, g	285 ± 41 a, b
500 to 0 ^a	2.9 ± 0.3 a, b	114 ± 5 e, g, h, i	246 ± 25 a, b
500 to 0 (2.5 min)	2.5 ± 0.2 a	103 ± 4 c, h, j, k	195 ± 13 b
0 to 500	2.9 ± 0.3 a, b	134 ± 9 a	385 ± 105 a, b
300 to 800	4.3 ± 0.5 b	112 ± 4 d, f, i, j	308 ± 42 a, b
800 to 300	3.5 ± 0.5 a, b	95 ± 4 b, k	210 ± 19 b

Linear ramps with a numeric range indicate the range (in $\mu\text{mol mol}^{-1}$) of $[\text{CO}_2]$ used for the RACiR technique. All ramps were run over 5 min unless otherwise noted. Data presented as means \pm s.e.m. with $n=6$. Identical lowercase letters indicate that means are not significantly different according to Tukey's HSD ($P > 0.05$). Bolded numbers indicate RACiR data that are significantly different than the standard $A-C_i$ curve. HSD, honestly significant difference; J_{max} , maximum rate of electron transport; RACiR, rapid $A-C_i$ response; RMSE, root mean square error of the model; s.e.m., standard error of the mean; $V_{c,max}$, maximum rate of Rubisco carboxylation; VPD, vapour pressure deficit. ^aRapid response was run without VPD control.

standard $A-C_i$ approach. Responses of stomatal conductance to changes in $[\text{CO}_2]_{\text{ref}}$ were broadly similar using the two measurement approaches (data not shown).

DISCUSSION

The RACiR technique generated gas exchange data on the biochemical limitations of photosynthesis, in 5 min or less, that were very similar to the traditional steady-state $A-C_i$ response. This is in contrast to typical times of 30 min or longer for C_3 species using the traditional steady-state $A-C_i$ response method. Interestingly, we found little effect of the direction of the CO_2 ramp on the response and curve fitting (Table 1 and Fig. 2), which is in contrast to common pitfalls in the traditional approach (Long & Bernacchi 2003). This may be because the measurement is sufficiently fast that it avoids complications from changes in enzyme activation, chloroplast movement or even potential problems from changing stomatal conductance and water potential (Long & Bernacchi 2003; Hanson *et al.* 2016). It is possible that the RACiR technique generates a more accurate snapshot of the biochemical and biophysical limitations of photosynthesis under a given environmental condition, but additional studies applying this technique will be required to test that hypothesis.

The RACiR technique works for two fundamental reasons: (1) the instrument design of the LI-6800 greatly minimizes lags between the reference and sample IRGAs and it can generate a constant ramp rate for CO_2 control and (2) it targets the CO_2 -limited and Rubisco regeneration co-limited regions of the $A-C_i$ response with high data density because these regions are particularly important for curve fitting (Sharkey *et al.* 2007; Gu *et al.* 2010), although other regions can be targeted or full CO_2 responses can be measured, with the latter increasing the measurement time. Using the standard configurations

of the LI-6800 set to automatically ramp $[\text{CO}_2]$ down and then up, between 30 s and 1 min of data are typically outside of the linear correction range and thus discarded. This causes a loss of 15 to 30 of the 150 data points collected over 5 min. That leaves over 120 data points for fitting, which is 10 times more than a traditional steady-state $A-C_i$ response, and traditional measurements are not typically focused on the co-limited regions. The large number of data points provided in the critical region generates great statistical power in the shortest period of time.

The minimum length of time required for a single RACiR ramp will depend on both the frequency of data collection and how optimally the co-limited region is captured (a larger range than necessary increases time but allows for more variation between plants and conditions). It is possible that increasing data collection to 1 Hz or faster would have eliminated statistically significant differences between the fits from the 2.5 min ramp and the 5 min ramps by keeping the number of data points higher. However, it may also be that the discarded data were in a more critical portion of the response or that the biochemistry was no longer in steady state. We did not pursue these questions for this report because the answers will be specific to species and environmental conditions. Therefore, we recommend pre-screening populations under environmental conditions of interest to identify the optimal $[\text{CO}_2]$ range and ensure that RACiR ramps are capturing a sufficient range of $[\text{CO}_2]$ to cover the CO_2 -limited and Rubisco-co-limited regions of the $A-C_i$ response. Other ranges may also be desirable for fitting additional parameters.

Even at 5 min, the speed of the RACiR technique puts it on a temporal scale appropriate for large-scale genotype screening of photosynthetic capacity in both natural and agricultural systems, especially when multiple instruments are used simultaneously. Allowing 1 min to move the gas exchange system between plants and 1 min for initial chamber stabilization (presuming leaf temperature, chamber light, and $[\text{CO}_2]$ are comparable), we can collect a 5 min ramp every 7 min (~70 plants per 8 h day per instrument). If genotype or species pre-screening is performed before a survey, even faster measurements could be possible, such as the 2.5 min ramp, which would allow ~100 plants to be measured per 8 h day per instrument.

Implications of rapid $A-C_i$ response – photosynthetic carbon metabolism

The lack of a statistically significant difference between the traditional steady-state and RACiR techniques implies that (1) carbon metabolism reaches a steady state nearly instantaneously (faster than we could measure via gas exchange using this method), allowing the use of the steady-state FvCB model, and (2) the gas exchange between the organelles and the air around the leaf achieves an effective steady-state condition at least as fast as we changed the gaseous environment, allowing measurements under dynamic conditions. Because of limitations in data collection frequency, we could not determine a rate of change in $[\text{CO}_2]$ that would push carbon metabolism or gas exchange into a non-steady state for $V_{c,max}$, although

200 $\mu\text{mol mol}^{-1} \text{ min}^{-1}$ does appear to compromise the estimation of J_{max} .

CONCLUSIONS

The RACiR technique is a breakthrough in our ability to measure biochemical limitations of photosynthesis, and to try to push photosynthetic carbon metabolism into a dynamic state. The timescale of RACiR means that logistical issues of setting up the measurements may be more restrictive than the time needed to take the measurements.

AUTHOR CONTRIBUTIONS

J.R.S. carried out the research. J.R.S. and D.T.H. wrote the paper with input from P.B.M., D.J.L., A.J.S. and D.K.M. D.T.H., P.B.M., D.J.L., A.J.S. and D.K.M. conceived of and developed the method.

CONFLICT OF INTEREST

D.T.H., P.B.M., D.J.L., A.J.S. and D.K.M. have a patent submitted on rapid response curves and survey measurements. D.K.M. has patents on the LI-6800.

ACKNOWLEDGMENTS

This research was partially supported by a Fulbright Canada scholarship to J.R.S. Fulbright Canada is a joint, bi-national, treaty-based organization created to encourage mutual understanding between Canada and the USA through academic and cultural exchange. Fulbright Canada is supported by the Canadian Government, through the Foreign Affairs Trade and Development Canada, by the US Government, through the Department of State, and by a diverse group of corporate sponsors, charitable trusts and university partners. It is governed by an independent board of directors and operates out of Ottawa. J.R.S. would also like to acknowledge scholarship support from the Natural Sciences and Engineering Research Council of Canada (NSERC). This work was also supported by funding to D.T.H. through the NSF EPSCoR Program under award no. IIA-1301346 at the University of New Mexico. P.B.M., D.J.L., A.J.S. and D.K.M. are indebted to the LI-COR development team for conceiving, designing and manufacturing the LI-6800 instruments that make this measurement possible. The team also thanks Jon M. Welles for creating the software controls for this method and Thomas J. Avenso for many insightful discussions and contributions. Any opinions, findings and conclusions or recommendations expressed in this material are those of the authors and do not necessarily reflect the views of the National Science Foundation.

REFERENCES

Araus J.L., Li J., Parray M.A.J. & Wang J. (2014) Phenotyping and other breeding approaches for a new green revolution. *Journal of Integrative Plant Biology* **56**, 422–424.

- Bellasio C., Beerling D.J. & Griffiths H. (2016a) Deriving C₄ photosynthetic parameters from combined gas exchange and chlorophyll fluorescence using an Excel tool: theory and practice. *Plant, Cell and Environment* **39**, 1164–1179.
- Bellasio C., Beerling D.J. & Griffiths H. (2016b) An Excel tool for deriving key photosynthetic parameters from combined gas exchange and chlorophyll fluorescence: theory and practice. *Plant, Cell and Environment* **39**, 1180–1197.
- Bishop K.A., Betzelberger A.M., Long S.P. & Ainsworth E.A. (2015) Is there potential to adapt soybean (*Glycine max* Merr.) to future [CO₂]? An analysis of the yield response of 18 genotypes in free-air CO₂ enrichment. *Plant, Cell and Environment* **38**, 1765–1774.
- Davis J.E., Arkebauer T.J., Norman J.M. & Brandle J.R. (1987) Rapid field measurement of the assimilation rate versus internal CO₂ concentration relationship in green ash (*Fraxinus pennsylvanica* Marsh.): the influence of light intensity. *Tree Physiology* **3**, 387–392.
- Duursma R.A. (2015) Plantecophys – an R package for analyzing and modelling leaf gas exchange data. *PLoS ONE* **10**, e0143346.
- Duursma R.A. & Medlyn B.E. (2012) MAESPA: a model to study interactions between water limitation, environmental drivers and vegetation function at tree and stand levels, with an example application to [CO₂] × drought interactions. *Geoscientific Model Development* **5**, 919–940.
- Ethier G.J. & Livingston N.J. (2004) On the need to incorporate sensitivity to CO₂ transfer conductance into the Farquhar–von Caemmerer–Berry leaf photosynthesis model. *Plant, Cell and Environment* **27**, 137–153.
- Farquhar G.D., von Caemmerer S. & Berry J.A. (1980) A biochemical model of photosynthetic CO₂ assimilation in leaves of C₃ species. *Planta* **149**, 78–90.
- Furbank R.T. & Tester M. (2011) Phenomics – technologies to relieve the phenotyping bottleneck. *Trends in Plant Science* **16**, 635–644.
- Gu L., Pallardy S.G., Tu K., Law B.E. & Wulschlegel S.D. (2010) Reliable estimation of biochemical parameters from C₃ leaf photosynthesis–intercellular carbon dioxide response curves. *Plant, Cell and Environment* **33**, 1852–1874.
- Hanson D.T., Stutz S.S. & Boyer J.S. (2016) Why small fluxes matter: the case and approaches for improving measurements of photosynthesis and (photo)respiration. *Journal of Experimental Botany* **67**, 3027–3039.
- Kull O. & Kruijff B. (1998) Leaf photosynthetic light response: a mechanistic model for scaling photosynthesis to leaves and canopies. *Functional Ecology* **12**, 767–777.
- Laik A. & Oja V. (1998) *Dynamics of Leaf Photosynthesis: Rapid-response Measurements and Their Interpretations*. CSIRO, Collingwood, VIC, Australia.
- Limousin J.M., Bickford C.P., Dickman L.T., Pangle R.E., Hudson P.J., Boutz A.L., ... McDowell N.G. (2013) Regulation and acclimation of leaf gas exchange in a piñon–juniper woodland exposed to three different precipitation regimes. *Plant, Cell and Environment* **36**, 1812–1825.
- Lobos G.A., Matus I., Rodriguez A., Romero-Bravo S., Araus J.L. & del Pozo A. (2014) Wheat genotypic variability in grain yield and carbon isotope discrimination under Mediterranean conditions assessed by spectral reflectance. *Journal of Integrative Plant Biology* **56**, 470–479.
- Long S.P. & Bernacchi C.J. (2003) Gas exchange measurements, what can they tell us about the underlying limitations to photosynthesis? Procedures and sources of error. *Journal of Experimental Botany* **54**, 2393–2401.
- Long S.P. & Hällgren J.E. (1993) Measurement of CO₂ assimilation by plants in the field and the laboratory. In *Photosynthesis and Production in a Changing Environment: A Field and Laboratory Manual* (eds Hall D.O., Scurlock J.M. O., Bolhar-Nordenkamp H.R., Leegood R.C. & Long S.P.), pp. 129–167. Chapman & Hall, London.
- McDermitt D.K., Norman J.M., Davis J.T., Ball T.M., Arkebauer T.J., Welles J.M. & Roemer S.R. (1989) CO₂ response curves can be measured with a field-portable closed-loop photosynthesis system. *Annals of Forestry Science* **46**, 416–420.
- Olesen K.W., Lawrence D.M., Bonan G.B., Dreiniak B., Huang M., Koven C.D., ... Yang Z.-L. (2013) *Technical Description of Version 4.5 of the Community Land Model (CLM)*. National Center for Atmospheric Research, Boulder, CO.
- Ray D.K., Mueller N.D., West P.C. & Foley J.A. (2013) Yield trends are insufficient to double global crop production by 2050. *PLoS ONE* **8**, e66428.
- Rogers A. (2014) The use and misuse of $V_{\text{c,max}}$ in earth system models. *Photosynthesis Research* **119**, 15–29.
- Serbin S.P., Singh A., Desai A.R., Dubois S.G., Jablonski A.D., Kingdon C.C., ... Townsend P.A. (2015) Remotely estimating photosynthetic capacity, and its response to temperature, in vegetation canopies using imaging spectroscopy. *Remote Sensing of Environment* **167**, 78–87.
- Sharkey T.D., Bernacchi C.J., Farquhar G.D. & Singsaas E.L. (2007) Fitting photosynthetic carbon dioxide response curves for C₃ leaves. *Plant, Cell and Environment* **30**, 1035–1040.
- von Caemmerer S. (2013) Steady-state models of photosynthesis. *Plant, Cell and Environment* **36**, 1617–1630.

Yendrek C.R., Tomaz T., Montes C.M., Cao Y., Morse A.M., Brown P.J., ... Ainsworth E.A. (2016) High-throughput phenotyping of maize leaf physiological and biochemical traits using hyperspectral reflectance. *Plant Physiology*. DOI:10.1104/pp.16.01447.

Received 23 November 2016; received in revised form 13 January 2017; accepted for publication 15 January 2017

[Correction added on 12 April 2017, after initial online publication on 1 March 2017: The below addendum was added for clarity of the method.]

ADDENDUM

Since submitting the manuscript it has come to our attention that with some instruments the relationship between A_{apparent} and reference $[\text{CO}_2]$ in empty chambers (equation 1) may be non-linear. In those instances a higher order polynomial fit will be needed to make the corrections, but the results are other-

wise unchanged. For an individual instrument the extent and shape of any non-linearity may be influenced by the CO_2 mole fraction of the gas chosen to set the span.

SUPPORTING INFORMATION

Additional Supporting Information may be found in the online version of this article at the publisher's web-site:

Figure S1. RACiR 500 to 0 ppm, empty chamber, uncorrected, full range

Figure S2. RACiR 500 to 0 ppm, empty chamber, uncorrected, linear range

Figure S3. RACiR 500 to 0 ppm, empty chamber, corrected

Figure S4. RACiR 500 to 0 ppm, leaf, reference CO_2

Figure S5. RACiR 500 to 0 ppm, leaf, Ci

Figure S6. RACiR 500 to 0 ppm, leaf, corrected